

Co-ordination chemistry of octamethyl-5,5'-di(2-pyridyl)ferrocene[†]

Beate Neumann,^a Ulrich Siemeling,^{*a} Hans-Georg Stammer,^a Udo Vorfeld,^a
 Johannes G. P. Delis,^b Piet W. N. M. van Leeuwen,^b Kees Vrieze,^b Jan Fraanje,^c
 Kees Goubitz,^c Fabrizia Fabrizi de Biani^d and Piero Zanello^d

^a Fakultät für Chemie, Universität Bielefeld, Universitätsstrasse 25, D-33615 Bielefeld, Germany

^b Anorganisch Chemisch Laboratorium, J. H. van't Hoff Instituut, Universiteit van Amsterdam, Nieuwe Achtergracht 166, NL-1018 WV Amsterdam, The Netherlands

^c Instituut voor Kristallografie, Amsterdams Instituut voor Moleculaire Studies, Universiteit van Amsterdam, Nieuwe Achtergracht 166, NL-1018 WV Amsterdam, The Netherlands

^d Dipartimento di Chimica, Università di Siena, Pian dei Mantellini 44, I-53100 Siena, Italy

The platinum complex $\{[PtCl_2(C_2H_4)]_2(dp f^*)\}$ **1** [$dp f^*$ = octamethyl-5,5'-di(2-pyridyl)ferrocene] has been obtained by the reaction of $dp f^*$ with $K[PtCl_3(C_2H_4)]$. The reaction of $dp f^*$ with $[Cu(NCCH_3)_4]^+[BF_4]^-$ afforded the copper complexes $[Cu(dp f^*)]^+[BF_4]^-$ **2** and $[Cu(dp f^*)]^+[CuCl_2]^-$ **3** as well as the ferrocenium salt $[dp f^*]^+[BF_4]^-$ **4**, depending on the stoichiometry. The crystal structures of **1–4** have been determined by X-ray diffraction. The $dp f^*$ acts as a bridging ligand in the case of **1** and as a *trans*-chelating ligand in **2** and **3**, which contain near-linear two-co-ordinate copper centres. Complex **3** shows a remarkably short, ligand-unsupported $Cu^I \cdots Cu^I$ contact [281.0(2) pm]. A cyclovoltammetric study of **2** revealed an unprecedentedly high anodic shift of the half-wave potential of the ferrocene moiety upon co-ordination of Cu^+ by $dp f^*$.

There is great current interest in ferrocene-based ligands. This is primarily due to the special stereo- and electro-chemical properties of the ferrocene group, which are the basis for a large variety of applications for such ligands, ranging, for example, from chemical sensors to asymmetric catalysis.¹ In this context, ferrocene-bearing pyridyl,² oligopyridyl³ and other aromatic *N*-donor groups^{2g,4} have emerged as a particularly important subclass. As part of an ongoing project concerned with the chemistry of pyridyl and oligopyridyl ligands bearing a ferrocene group as redox spectator, we have synthesized octamethyl-5,5'-di(2-pyridyl)ferrocene ($dp f^*$).⁵ The unmethylated analogue 1,1'-di(2-pyridyl)ferrocene (dpf) has already proved to be a very versatile ligand, which can accommodate a wide range of co-ordination geometries.^{2h,6} It can act as a mono- or as a bidentate ligand. In the latter case it may either co-ordinate two metal centres in a bridging or one metal centre in a chelating mode. Interestingly, in the latter case, a *cis*^{2h} or a *trans*⁶ arrangement of the pyridyl moieties at the chelated metal centre can be realised, so that with dpf *N*–*M*–*N* 'bite' angles close to 90 and 180° have been observed. We have investigated the co-ordination behaviour of $dp f^*$ towards palladium, platinum and copper. Part of this study has been briefly communicated.^{2a}

Results and Discussion

Like its unmethylated analogue dpf , $dp f^*$ reacted cleanly with 2 equivalents of $K[PtCl_3(C_2H_4)]$ (Zeise's salt) in dichloromethane at room temperature, giving the expected product $\{[PtCl_2(C_2H_4)]_2(dp f^*)\}$ **1** in 80% yield. A single-crystal X-ray diffraction study performed for **1** confirms that the $dp f^*$ unit bridges the two platinum centres (Fig. 1). Bond lengths and angles are unexceptional (Table 1).

The structure is quite similar to that of $\{[PtCl_2(C_2H_4)]_2(dp f)\}$.^{2h} It has molecular (and crystallographic) C_2 symmetry. Each platinum atom is co-ordinated by one nitrogen, two chlorine and two carbon atoms; its deviation from the plane defined by the nitrogen and the two chlorine atoms is *ca.* 10 pm. Each ethylene ligand is in an approximately perpendicular orientation to the respective Cl–Cl–N–Pt co-ordination plane. The

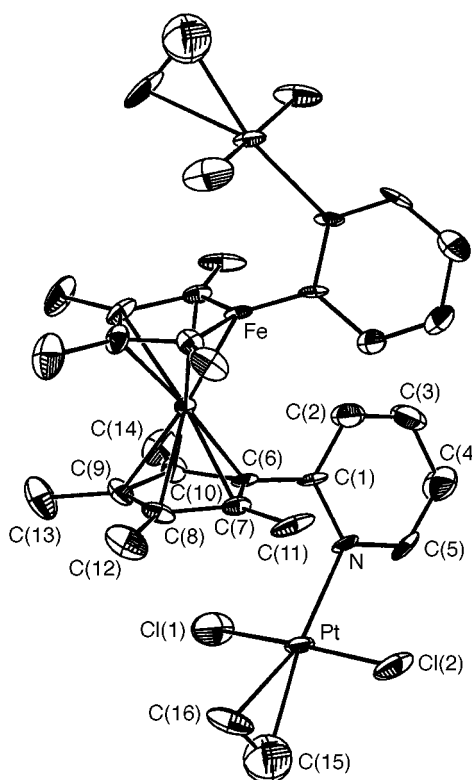


Fig. 1 Molecular structure of complex **1**

dihedral angle between the plane defined by Pt, C(15) and C(16) and the best plane for Pt, Cl(1), Cl(2) and N is 93.7°, and the relevant Cl–Pt–C torsion angles are close to 90°. The Cl–Pt–N and Cl–Pt–C angles, which are identical within experimental error, are approximately 90°; the Cl–Pt–Cl angles [174.9(2)°] deviate slightly from linearity. The co-ordination of the two $PtCl_2(C_2H_4)$ fragments leads to pronounced angular distortions of the $dp f^*$ framework. The best planes of the cyclopentadienyl ring and the pyridyl ring attached to it intersect each other at an angle of 72.1°, which is decisively more than the corresponding values of 33.3 and 36.9° found for

[†] Non-SI unit employed: cal \approx 4.184 J.

Table 1 Selected bond lengths (pm) and angles (°) with estimated standard deviations in parentheses for the platinum complex **1**

Pt–Cl(1)	227.1(6)	C(5)–N	133(2)
Pt–Cl(2)	229.6(5)	C(6)–C(7)	144(2)
Pt–C(15)	218(2)	C(6)–C(10)	144(2)
Pt–C(16)	219(2)	C(7)–C(8)	146(2)
Pt–N	208(1)	C(7)–C(11)	148(2)
Fe–C(6)	207(1)	C(8)–C(9)	142(2)
Fe–C(7)	209(1)	C(8)–C(12)	148(2)
Fe–C(8)	208(1)	C(9)–C(10)	145(2)
Fe–C(9)	208(1)	C(9)–C(13)	149(2)
Fe–C(10)	206(1)	C(10)–C(14)	146(2)
C(1)–C(6)	145(2)	C(15)–C(16)	143(4)
C(1)–N	137(2)		
Cl(1)–Pt–C(15)	87.4(7)	Cl(2)–Pt–N	90.1(4)
Cl(1)–Pt–C(16)	91.5(7)	C(15)–Pt–C(16)	38(1)
Cl(1)–Pt–N	90.0(4)	C(15)–Pt–N	164.8(9)
Cl(2)–Pt–C(15)	91.2(7)	C(16)–Pt–N	157.0(8)
Cl(2)–Pt–C(16)	90.3(7)		

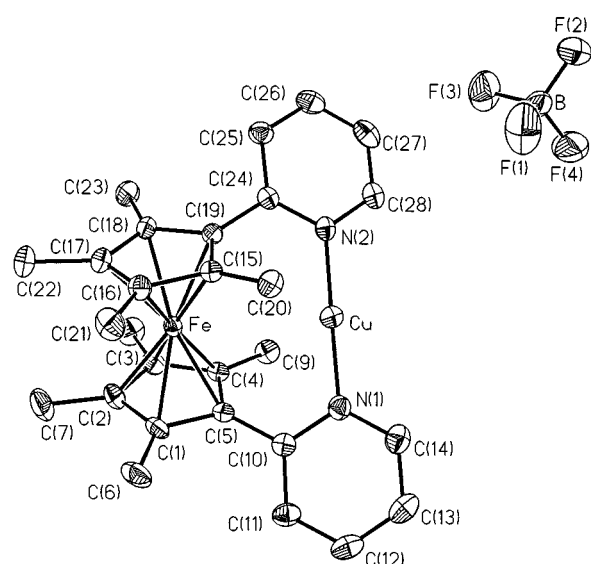


Fig. 2 Molecular structure of complex **2**

uncomplexed dpf*. The two cyclopentadienyl rings are no longer coplanar in **1**, forming an angle of 6.1°. The best planes of the two pyridyl units intersect each other at an angle of 44.4°, which is a drastic deviation from the corresponding value of only 9.9° in free dpf*.

In an attempt to synthesize a chelate complex of dpf*, this was stirred with an equimolar amount of [Pd(Me)Cl(cod)] (cod = cycloocta-1,5-diene) in toluene solution. However, no reaction occurred, even at higher temperatures. This is in contrast to the behaviour of dpf, which reacts cleanly and swiftly with this palladium compound at room temperature giving the *cis*-chelate complex [Pd(Me)Cl(dpf)] in almost quantitative yield.^{2h} According to this result, a *cis*-chelating co-ordination of a metal–ligand fragment by dpf* is comparatively unfavourable, which may be ascribed primarily to the steric influence of the methyl groups in the vicinity of the pyridyl units.

In contrast, the *trans*-chelating co-ordination mode of dpf* could be realised straightforwardly by utilising a small, 'naked' metal cation, namely Cu^I, which is known to prefer a quasi-linear two-co-ordinate environment with moderately bulky aromatic *N*-donor ligands.⁷ When a solution of equimolar amounts of [Cu(NCCH₃)₄]⁺[BF₄][−] and dpf* in dichloromethane was stirred at room temperature the expected *trans*-chelate complex [Cu(dpfp*)]⁺[BF₄][−] **2** was obtained in good yield as a dark red crystalline solid after standard work-up. The molecular structure **2** was determined by a single-

Table 2 Selected bond lengths (pm) and angles (°) with estimated standard deviations in parentheses for the copper complex **2**

Fe–C(1)	206.9(3)	C(3)–C(4)	142.2(4)
Fe–C(2)	207.1(3)	C(3)–C(8)	149.5(5)
Fe–C(3)	207.4(3)	C(4)–C(5)	144.8(4)
Fe–C(4)	207.0(3)	C(4)–C(9)	149.4(4)
Fe–C(5)	207.2(3)	C(5)–C(10)	147.5(4)
Fe–C(15)	206.5(3)	C(15)–C(16)	143.1(4)
Fe–C(16)	207.7(3)	C(15)–C(19)	145.1(4)
Fe–C(17)	207.8(3)	C(15)–C(20)	149.8(4)
Fe–C(18)	207.4(3)	C(16)–C(17)	142.0(4)
Fe–C(19)	205.7(3)	C(16)–C(21)	149.4(4)
N(1)–C(10)	135.2(4)	C(17)–C(18)	143.1(4)
N(1)–C(14)	135.2(4)	C(17)–C(22)	150.3(4)
N(2)–C(24)	135.1(4)	C(18)–C(19)	142.8(4)
N(2)–C(28)	136.5(4)	C(18)–C(23)	149.7(4)
C(1)–C(2)	143.3(5)	C(19)–C(24)	147.5(4)
C(1)–C(5)	143.8(4)	B–F(1)	137.2(5)
C(1)–C(6)	149.3(4)	B–F(2)	137.1(6)
C(2)–C(3)	142.7(5)	B–F(3)	137.6(6)
C(2)–C(7)	149.6(5)	B–F(4)	137.1(6)
C(5)–C(1)–C(6)	126.3(3)	C(19)–C(15)–C(20)	128.7(3)
C(5)–C(4)–C(9)	128.9(3)	C(19)–C(18)–C(23)	126.3(3)
C(1)–C(5)–C(10)	124.6(3)	C(15)–C(19)–C(24)	127.1(3)
C(4)–C(5)–C(10)	126.5(3)	C(18)–C(19)–C(24)	123.5(3)

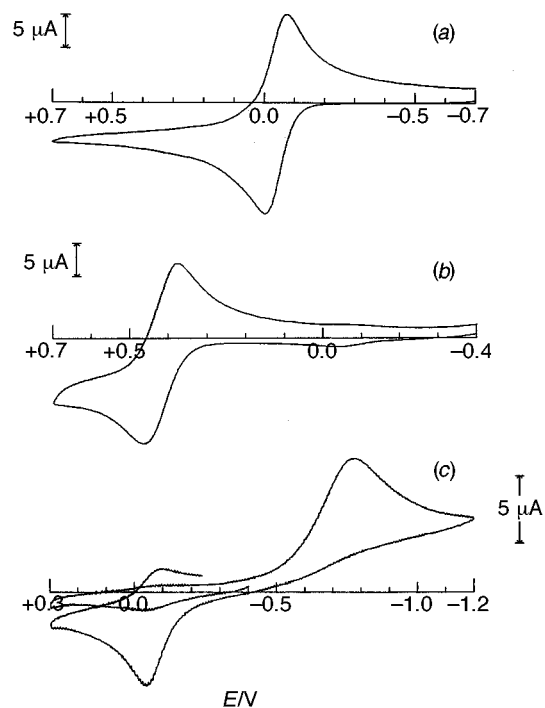


Fig. 3 Cyclic voltammetric responses recorded at a platinum electrode in CH₂Cl₂ solutions containing [NBu₄][PF₆] (0.2 mol dm^{−3}) and (a) dpf* (1.5 × 10^{−3} dm^{−3}), (b, c) complex **2** (1.3 × 10^{−3} dm^{−3}). Scan rate 0.1 V s^{−1}

crystal X-ray diffraction study (Fig. 2). Bond lengths and angles are collected in Table 2. The [Cu(dpfp*)]⁺ ion exhibits Cu–N distances of 186.2(3) pm, short in comparison to corresponding distances in three- and four-co-ordinate copper(I) compounds.⁸ The copper centre is linear two-co-ordinate with a N–Cu–N angle of 178.28(11)°. Again, dihedral angles differ markedly from those of uncomplexed dpf* (see above). The best planes of the cyclopentadienyl rings form an angle of 5.8°, those of the pyridyl rings intersect each other at an angle of 32.1°, and the cyclopentadienyl–pyridyl dihedral angles are 48.0 and 50.9°.

The interaction between the ferrocene unit and the co-ordinated copper ion was investigated by electrochemical techniques. Fig. 3 compares the cyclic voltammetric behaviour of

Table 3 Formal electrode potentials (in V, vs. SCE) and peak-to-peak separations (in mV) for the oxidation process of the present complexes in CH₂Cl₂ solution^a

Complex	$E^{\circ'}$ _{ox}	ΔE_p ^b
dpf*	−0.04	72
2	+0.42	90
[Fe(C ₅ Me ₅) ₂]	−0.15	78
[Fe(C ₅ H ₅) ₂]	+0.39	80

^a [NBu₄][PF₆] supporting electrolyte (0.2 mol dm^{−3}). ^b Measured at 0.1 V s^{−1}.

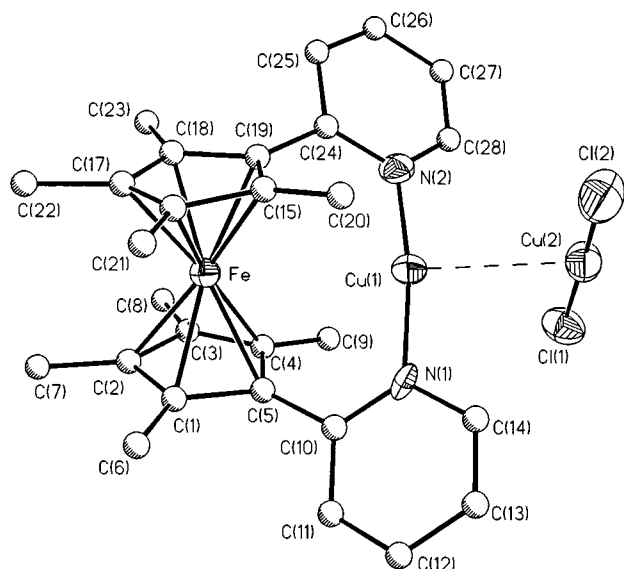


Fig. 4 Molecular structure of complex **3**

dpf* with that of its copper(I) complex **2**. Free dpf* displays the expected facile oxidation typical of permethylated ferrocenes. Controlled-potential coulometry ($E_w = 0.3$ V) consumed one electron per molecule, causing the original orange solution ($\lambda_{\text{max}} = 474$ nm) to turn olive-green and to exhibit a shoulder in the range 600–700 nm, typical of ferrocenium species, close to a broad and intense charge-transfer (CT) absorption at $\lambda_{\text{max}} = 787$ nm. In confirmation of the electrochemical reversibility of the one-electron removal, the olive-green solution showed a cyclic voltammetric profile quite complementary to that shown in Fig. 3(a). Analysis⁹ of the cyclic voltammetric responses of dpf* with scan rates varying from 0.02 to 1.00 V s^{−1} is consistent with a simple, electrochemically reversible process, thus precluding the crystallographically confirmed absence of significant structural reorganisations accompanying the one-electron removal (see below).

As Fig. 3(b) illustrates, complex **2** also undergoes a similar anodic process, but at significantly higher potentials. Exhaustive one-electron oxidation ($E_w = 0.7$ V) of the original red-orange solution ($\lambda_{\text{max}} = 504$ nm) afforded a yellow-brown solution, which again displayed a minor ferrocenium absorption at $\lambda_{\text{max}} = 658$ together with an intense CT band at $\lambda_{\text{max}} = 805$ nm. As deducible from Fig. 3(c), **2** also undergoes an irreversible cathodic process at $E_p = -0.78$ V, which generates in the reverse scan the voltammetric profile of free dpf*. We confidently assume this process to be due to the Cu^I–Cu⁰ reduction, which is complicated by decomplexation of dpf*. No clean Cu^I–Cu^{II} oxidation was detected, but a broad, ill shaped anodic peak at about 0.9 V.

Table 3 compiles the formal electrode potentials of the ferrocene-centered oxidation of the present complexes. Two main electronic effects are easily detectable: (i) with respect to decamethylferrocene, substitution of two methyl groups by two pyridyl units in dpf* makes the oxidation more difficult by

Table 4 Selected bond lengths (pm) and angles (°) with estimated standard deviations in parentheses for the copper complex **3**

Fe–C(1)	208(2)	C(1)–C(6)	148(2)
Fe–C(2)	209(2)	C(2)–C(3)	147(2)
Fe–C(3)	210(2)	C(2)–C(7)	151(2)
Fe–C(4)	207(2)	C(3)–C(4)	137(2)
Fe–C(5)	211(2)	C(3)–C(8)	152(2)
Fe–C(15)	210(2)	C(4)–C(5)	145(2)
Fe–C(16)	204(2)	C(4)–C(9)	153(2)
Fe–C(17)	203(3)	C(5)–C(10)	145(2)
Fe–C(18)	204(2)	C(15)–C(16)	145(2)
Fe–C(19)	204(2)	C(15)–C(19)	147(2)
Cu(2)–Cl(1)	212.3(7)	C(15)–C(20)	149(2)
Cu(2)–Cl(2)	206.6(7)	C(16)–C(17)	137(2)
N(1)–C(10)	133(2)	C(16)–C(21)	153(2)
N(1)–C(14)	136(2)	C(17)–C(18)	138(3)
N(2)–C(24)	137(2)	C(17)–C(22)	153(2)
N(2)–C(28)	132(2)	C(18)–C(19)	143(3)
C(1)–C(2)	145(2)	C(18)–C(23)	151(3)
C(1)–C(5)	146(2)	C(19)–C(24)	148(2)
C(5)–C(1)–C(6)	125(2)	C(19)–C(15)–C(20)	132(2)
C(5)–C(4)–C(9)	128(2)	C(19)–C(18)–C(23)	122(2)
C(1)–C(5)–C(10)	127(2)	C(15)–C(19)–C(24)	125(2)
C(4)–C(5)–C(10)	128(2)	C(18)–C(19)–C(24)	128(2)

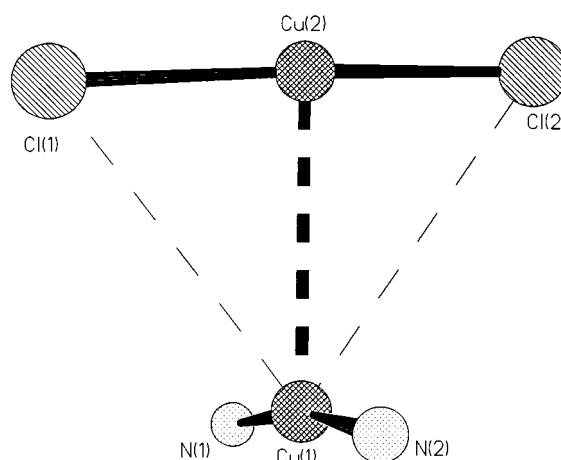


Fig. 5 View of the co-ordination spheres of the copper centres in complex **3**

about 0.1 V; (ii) complexation of copper(I) causes the oxidation to shift to a more positive potential by about 0.5 V, which could render the present system one of the most effective redox sensors for copper ions presently known.¹⁰ The magnitude of the anodic shift, which is indicative of a remarkably strong interaction between the ferrocene unit and the copper(I) ion, is undoubtedly due to their close proximity (the Fe...Cu distance is only 323 pm).

All attempts to co-ordinate two dpf* ligands to one copper(I) centre by treating [Cu(NCCH₃)₄]⁺[BF₄][−] with 2 equivalents of dpf* were unsuccessful, yielding only mixtures of complex **2** and free dpf*. In one instance, however, the unexpected product [Cu(dpf*)]⁺[CuCl₂][−] **3** was obtained in moderate yield. The formation of this species involved a reaction of the solvent dichloromethane, since no other sources of Cl were present in the reaction mixture. A single-crystal X-ray diffraction study for **3** showed that it contained two copper(I) centres in a slightly distorted linear two-co-ordinate environment (Fig. 4). Bond lengths and angles are collected in Table 4. The dihedral angle formed by the best planes of the two cyclopentadienyl rings is 5.9°, the corresponding angle between the best planes of the two pyridyl groups is 46.3°, and the cyclopentadienyl–pyridyl dihedral angles are 44.8 and 46.8°. An important feature of the structure of **3** is the short distance between the two copper

centres of only 281.0(2) pm. The co-ordination axes of the anion and the cation, which are both slightly bent [N(1)–Cu(1)–N(2) 171.4(6), Cl(1)–Cu(2)–Cl(2) 176.9(3)°], are approximately perpendicular to each other [torsion angles: N(1)–Cu(1)–Cu(2)–Cl(1) 85.5, N(2)–Cu(1)–Cu(2)–Cl(2) 89.4°] (Fig. 5).

It is instructive to compare the structure of complex **3** with that of **2**, which contains a co-ordinatively innocent anion. The interaction of the [CuCl₂][–] anion with the nitrogen-co-ordinated copper centre leads to an increase of the Fe...Cu distance from 323.1 pm in the tetrafluoroborate **2** to 329.2 pm in the dichlorocuprate **3**, and also to an elongation of the copper–nitrogen bonds from 186.2 to 192.5 pm (mean) together with a bending of the N–Cu–N axis by *ca.* 6°. The [CuCl₂][–] anion appears to pull the nitrogen-co-ordinated copper ion away from the ferrocene moiety. There are no appreciable secondary interactions between the nitrogen-co-ordinated copper centre and the chlorine atoms of the anion, since both copper–chlorine distances [Cu(1)–Cl(1) 337, Cu(1)–Cl(2) 358 pm] are considerably larger than the sum of the van der Waals radii of Cu (140 pm) and Cl (175 pm).¹¹ There is no indication for intermolecular interactions of the chlorine-co-ordinated copper centre, its shortest intermolecular contact (Cu...C 398 pm) being that to the methyl group attached to C(1) of a neighbouring [Cu(dpf*)]⁺ unit.

To the best of our knowledge, [Cu(dpf*)]⁺[CuCl₂][–] **3** is only the second example so far of a complex which contains a short ligand-unassisted Cu^I...Cu^I contact, the first example being the trinuclear species [(CuL)₃] {HL = 2-[pyrazol-3(5)-pyridine]}, which crystallises as a dimer showing two close metal–metal contacts between the two associated trinuclear units in the absence of any supportive bridging ligation [*d*(Cu–Cu) 290.5(3) pm].¹² Such close contacts may be interpreted in terms of a weak bonding interaction between the two d¹⁰ metal centres.

Attractive interactions between formally closed-shell metal centres (s² or d¹⁰) are well documented for several metals.¹³ However, whereas the body of evidence is especially large in the case of gold(I), where the term ‘aurophilicity’ has been coined to describe this special kind of metal–metal bonding interaction,¹⁴ the question of whether a similar metallophilicity¹⁵ exists in the case of the other two coinage metals, copper and silver, is still a matter of controversy. For example, the presence of such d¹⁰–d¹⁰ bonding interactions has been disputed on theoretical grounds for the dinuclear complexes {[M(CH₃C₆H₄NCH–NC₆H₄CH₃)]₂} in spite of rather short metal–metal distances [247.7(2)/270.5(1) pm for M = Cu/Ag], which were therefore attributed to the ligand architecture.¹⁶ A most instructive case is that of the trinuclear copper complex {[Cu(CH₃C₆H₄–N₅C₆H₄CH₃)]₃}, where the metal centres have an average distance of only 235 pm.¹⁷ The existence of a cuprophilic interaction between them has both been supported¹⁸ and refuted¹⁹ at various levels of theory.

Generally, weak metallophilic effects are easily blurred or even overruled by other secondary interactions. Even for gold(I), where aurophilic bonding can be as strong as 11 kcal mol^{–1},²⁰ it has been noted that metallophilic energy minima may be rather shallow.²¹ The same is assumed to be true for copper(I), so that crystal packing forces²² may very well overrule weak cuprophilic interactions. In comparison, this appears to be the case for the complex [Cu(NC₅H₂Me₃-2,4,6)₂]⁺[CuCl₂][–],^{7b,d} the Cu^I...Cu^I distance of 361.1(2) pm being *ca.* 80 pm longer than that in [Cu(dpf*)]⁺[CuCl₂][–] **3**, although the co-ordination parameters of the respective copper(I) centres are quite similar for both complexes. Closer inspection reveals that the packing of the [Cu(NC₅H₂Me₃-2,4,6)₂]⁺ units in the crystal, which involves stacking of neighbouring collidine ligands with a closest inter-ring distance of 348 pm [calculated from crystallographic data given in ref. 7(d)], prohibits a closer approach of the copper centres.

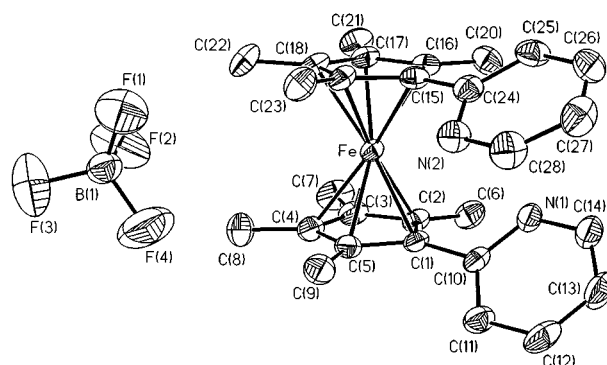


Fig. 6 Molecular structure of complex **4**

Table 5 Selected bond lengths (pm) and angles (°) with estimated standard deviations in parentheses for the ferrocenium salt **4**

Fe–C(1)	207.4(3)	C(3)–C(7)	150.7(5)
Fe–C(2)	208.3(3)	C(4)–C(5)	142.3(5)
Fe–C(3)	210.0(3)	C(4)–C(8)	148.6(5)
Fe–C(4)	212.9(4)	C(5)–C(9)	149.1(5)
Fe–C(5)	210.3(3)	C(15)–C(16)	145.0(5)
Fe–C(15)	207.0(3)	C(15)–C(19)	143.9(5)
Fe–C(16)	208.9(3)	C(15)–C(24)	147.9(5)
Fe–C(17)	212.1(3)	C(16)–C(17)	143.5(5)
Fe–C(18)	211.6(3)	C(16)–C(20)	149.1(5)
Fe–C(19)	209.1(3)	C(17)–C(18)	141.4(5)
N(1)–C(10)	134.6(5)	C(17)–C(21)	149.5(5)
N(1)–C(14)	134.3(5)	C(18)–C(19)	142.6(5)
N(2)–C(24)	134.8(5)	C(18)–C(22)	150.4(5)
N(2)–C(28)	134.0(5)	C(19)–C(23)	149.6(5)
C(1)–C(2)	144.5(5)	B–F(1)	138.2(5)
C(1)–C(5)	144.0(5)	B–F(2)	136.4(6)
C(2)–C(3)	142.1(5)	B–F(3)	135.7(6)
C(2)–C(6)	149.2(5)	B–F(4)	135.3(6)
C(3)–C(4)	142.8(5)		
C(2)–C(1)–C(10)	125.3(3)	C(16)–C(15)–C(24)	126.1(3)
C(5)–C(1)–C(10)	127.0(3)	C(19)–C(15)–C(24)	126.3(3)
C(1)–C(2)–C(6)	127.1(3)	C(15)–C(16)–C(20)	128.5(3)
C(1)–C(5)–C(9)	127.0(3)	C(15)–C(19)–C(23)	127.2(3)

The formation of [Cu(dpf*)]⁺[CuCl₂][–] **3** was irreproducible,‡ even when the stoichiometry of the reaction was inverted in order to take account of the copper:dpf* ratio of 2:1 in the serendipitous product. In the reaction of 2 equivalents of [Cu(NCCH₃)₄]⁺[BF₄][–] with dpf* oxidation of the latter occurred, and [dpf*]⁺[BF₄][–] **4** was isolated in good yield. No formation of a product containing the [Cu(dpf*)]²⁺ dication was observed, although this species can be generated by electrochemical oxidation of [Cu(dpf*)]⁺ and appears to be chemically stable. In view of the anodic shift of the ferrocene-centred oxidation in **2** (see above), it is likely that more powerful oxidising agents are needed.

A single-crystal X-ray diffraction study of the ferrocenium salt **4** (Fig. 6) reveals that, with respect to dpf*, the oxidation does not lead to any appreciable structural changes. Bond lengths and angles are collected in Table 5. The mean distance between the iron centre and the cyclopentadienyl ring C atoms increases slightly, but significantly, from 207 to 210 pm upon oxidation, whereas the average C–C bond length in the cyclopentadienyl rings (143 pm) remains the same. This is in accord with findings concerning other persubstituted ferrocenes.²³

‡ Attempts to obtain complex **3** more straightforwardly by the reaction of dpf* with copper(I) chloride in dichloromethane or acetonitrile or mixtures of both were unsuccessful.

Table 6 Crystallographic data for compounds 1–4

Compound	1·CH ₂ Cl ₂	2	3	4
Formula	C ₃₃ H ₄₂ Cl ₄ FeN ₂ Pt ₂	C ₂₈ H ₃₂ BCuF ₄ FeN ₂	C ₂₈ H ₃₂ Cl ₂ Cu ₂ FeN ₂	C ₂₈ H ₃₂ BF ₄ FeN ₂
<i>M</i>	1040.5	602.8	650.4	539.2
Crystal system	Monoclinic	Triclinic	Orthorhombic	Monoclinic
Space group	<i>P</i> 2/ <i>c</i>	<i>P</i> $\bar{1}$	<i>Pna</i> 2 ₁	<i>P</i> 2 ₁ / <i>n</i>
<i>a</i> /Å	9.436(2)	7.586(2)	21.238(4)	8.622(2)
<i>b</i> /Å	11.208(2)	11.338(3)	8.7730(10)	24.596(4)
<i>c</i> /Å	17.980(4)	16.041(3)	14.2570(10)	11.911(4)
α /°		73.06(2)		
β /°	97.44(2)	89.37(2)		94.11(2)
γ /°		75.22(2)		
<i>U</i> /Å ³	1885.5(8)	1273.2(5)	2656.4(6)	2519.4(11)
<i>Z</i>	2	2	4	4
<i>D_c</i> /g cm ^{−3}	1.98	1.57	1.63	1.42
λ /Å (graphite monochromated)	1.5418 (Cu-K α)	0.710 73 (Mo-K α)	0.710 73 (Mo-K α)	0.710 73 (Mo-K α)
μ /mm ^{−1}	21.04	1.455	2.347	0.648
<i>F</i> (000)	1076	620	1328	1124
θ Range/°	3.9–75.8	1.95–30.00	1.92–25.04	1.66–27.56
Scan type	ω	Wyckoff	ω	ω
Standard reflections	2 every hour	3 of 50 measured	3 of 100 measured	3 of 100 measured
Index ranges	−11 ≤ <i>h</i> ≤ 11, 0 ≤ <i>k</i> ≤ 14, 0 ≤ <i>l</i> ≤ 22	0 ≤ <i>h</i> ≤ 10, −15 ≤ <i>k</i> ≤ 15, −22 ≤ <i>l</i> ≤ 22	0 ≤ <i>h</i> ≤ 25, −10 ≤ <i>k</i> ≤ 10, 0 ≤ <i>l</i> ≤ 16	0 ≤ <i>h</i> ≤ 11, 0 ≤ <i>k</i> ≤ 32, −15 ≤ <i>l</i> ≤ 15
Independent reflections	3899	7429	2423	5785
Data, restraints, parameters	3456, 0, 190	7388, 0, 343	2423, 1, 184	5761, 0, 333
<i>R</i> ^a (number of reflections used for)	0.080 (3456)	0.053 (6068)	0.069 (1186)	0.059 (4008)
Largest Δ /σ	0.12	0.00	0.00	0.00
Largest difference peak and hole/e Å ^{−3}	4.5, −3.9 ^b	0.5, −0.9	0.6, −0.5	0.5, −0.7

^a Conventional $R = \Sigma ||F_o| - |F_c|| / \Sigma |F_o|$. ^b In the vicinity of the heavy atoms.

Experimental

X-Ray crystallography

Complex 1·CH₂Cl₂. A crystal with dimensions 0.35 × 0.60 × 0.65 mm was used for data collection at room temperature on an Enraf-Nonius CAD-4 diffractometer. Corrections for Lorentz-polarisation effects were applied. An absorption correction was performed with the program ABSCAL²⁴ using ψ scans of the [1 0 8] reflection, with coefficients in the range 1.01–2.02. 3456 Reflections were above the significance level of $2.5\sigma(I)$. The structure was solved by the PATTY option of the DIRDIF 94 program system.²⁵ The hydrogen atoms were calculated and kept fixed during refinement with $U = 0.10 \text{ \AA}^2$. The hydrogen atoms of the ethylene moiety and the solvent molecule were not included in the refinement. The positions of the solvent atoms were not refined. Full-matrix least-squares refinement on F was carried out isotropically for the solvent atoms and the hydrogen atoms and anisotropically for all other atoms. A weighting scheme $w = 1/\{22.0 + 0.01[\sigma(F_o)]^2 + 0.001[\sigma(F_o)]^{-1}\}$ was used leading to an R' value of 0.093. The secondary isotropic extinction coefficient²⁶ refined to a value of 0.16(1). The anomalous scattering of Pt, Fe and Cl was taken into account. All calculations were performed with XTAL,²⁷ unless stated otherwise. The asymmetric unit contains half a molecule, while the positions of the solvent atoms have an occupancy factor of 0.5. Pertinent crystallographic data are collected in Table 6.

Complexes 2–4. Crystals with dimensions $1.20 \times 0.40 \times 0.10$ (**2**), $0.30 \times 0.10 \times 0.10$ (**3**) and $0.50 \times 0.40 \times 0.15$ mm (**4**), respectively, were used for data collection at 173(2) K on a Siemens P2(1) four-circle diffractometer. The structures were solved by direct methods. Programs used were Siemens SHELXTL PLUS²⁸ and SHELXL 93.²⁹ Full-matrix least-squares refinement on F^2 was carried out anisotropically for the non-hydrogen atoms and isotropically for the hydrogen atoms, except in the case of complex **3**, where atoms heavier than carbon were refined anisotropically and all other atoms isotropically. Weighting schemes used were $w = [\sigma^2(F_o^2) + (0.0666P)^2 + 2.3888P]^{-1}$ in the case of **2**, $w = [\sigma^2(F_o^2) + (0.0319P)^2]^{-1}$ in the case of **3** and $w = [\sigma^2(F_o^2) + (0.0676P)^2 + 3.0594P]^{-1}$ in the case of **4**, where $P = (F_o^2 + 2F_c^2)/3$ in all cases, leading to R' values (all data) of 0.163, 0.140 and 0.179 for **2**, **3** and **4**, respectively. All three structures developed routinely. Pertinent crystallographic data are collected in Table 6.

CCDC reference number 186/746.

Electrochemistry

Materials and apparatus used for the electrochemical investigations have been described elsewhere.³⁰ All potential values are referred to the saturated calomel electrode (SCE).

General

All reactions were performed in an inert atmosphere (purified argon or dinitrogen) by using standard Schlenk and cannula techniques or a conventional glove-box. Solvents and reagents were rigorously dried and purified by standard procedures. The NMR spectra were recorded at 300 K with a Bruker AMX 300 or DRX 500 spectrometer operating at 300.13 and 500.13 MHz, respectively, for ¹H. Elemental analyses were performed by the Microanalytical Laboratory of the Universität Bielefeld, or by Dornis und Kolbe, Mikroanalytisches Laboratorium, Mülheim a. d. Ruhr, Germany.

Syntheses

[PtCl₂(C₂H₄)(dpf*)] 1. A solution of K[PtCl₂(C₂H₄)] (100 mg, 0.28 mmol) and dpf* (90 mg, 0.20 mmol) in dichloromethane (30 cm³) was stirred for 1 h. The red solution was filtered

and the volume of the filtrate reduced to 5 cm³. Diethyl ether was added and dark red complex **1** (167 mg, 80%) was collected by centrifugation (Found: C, 35.1; H, 3.7; N, 2.5. C₃₂H₄₀Cl₂FeN₂Pt₂·CH₂Cl₂ requires C, 35.2; H, 3.8; N, 2.5%). δ_H (300.1 MHz, CDCl₃) 1.83 and 2.01 (2 s, 2 × 12 H, Me), 4.55 [s with ¹⁹⁵Pt satellites, J (PtH) 49 Hz, 8 H, C₂H₄], 7.28, 7.47, 7.64 and 8.75 (4 m, 4 × 2 H, pyridyl CH); δ_C (75.5 MHz, CDCl₃) 9.9 and 12.7 (Me), 74.0 (C₂H₄), 81.5, 82.7 and 88.1 (C₅ ring), 122.9, 132.2, 138.2 and 151.7 (pyridyl CH), 160.7 (quaternary pyridyl C).

[Cu(dpfp*)]⁺[BF₄][−] 2. A solution of [Cu(NCCH₃)₄]⁺[BF₄][−] (252 mg, 0.80 mmol) and dpfp* (362 mg, 0.80 mmol) in dichloromethane (20 cm³) was stirred for 14 h. Volatile components were removed *in vacuo*. The dark brownish red residue was dissolved in the minimum volume of dichloromethane. Vapour-phase diffusion of diethyl ether into this solution afforded complex **2** (347 mg, 72%) as dark red needles (Found: C, 56.2; H, 5.3; N, 4.5. C₂₈H₃₂BCuF₄FeN₂ requires C, 55.8; H, 5.35; N, 4.65%). δ_H (500.1 MHz, CDCl₃) 1.54 and 1.75 (2 br s, 2 × 12 H, Me), 7.31, 7.43, 7.77 and 9.13 (4 m, 4 × 2 H, pyridyl CH); δ_C (125.8 MHz, CDCl₃) 9.7 and 11.6 (Me), 80.2, 82.6 and 85.8 (C₅ ring), 123.0, 127.5, 138.1 and 151.6 (pyridyl CH), 158.7 (quaternary pyridyl C).

[Cu(dpfp*)]⁺[CuCl₂][−] 3. A solution of dpfp* (362 mg, 0.80 mmol) in dichloromethane (5 cm³) was added to a solution of [Cu(NCCH₃)₄]⁺[BF₄][−] (126 mg, 0.40 mmol) in dichloromethane (10 cm³) with vigorous stirring. After 12 h volatile components were removed *in vacuo* leaving a viscous, brownish red oil, which was dissolved in the minimum volume of dichloromethane. Vapour-phase diffusion of *n*-pentane into this solution afforded complex **3** (66 mg, 43%) as red crystals (Found: C, 51.65; H, 5.1; N, 4.3. C₂₈H₃₂Cl₂Cu₂FeN₂ requires C, 51.7; H, 5.0; N, 4.3%). δ_H (500.1 MHz, CDCl₃) 1.64 and 1.86 (2 s, 2 × 12 H, Me), 7.25, 7.40, 7.74 and 9.42 (4 br s, 4 × 2 H, pyridyl CH); δ_C (125.8 MHz, CDCl₃) 9.7 and 12.0 (Me), 80.2, 82.6 and 85.6 (C₅ ring), 122.5, 127.7, 137.7, 151.9 (pyridyl CH), 158.7 (quaternary pyridyl C).

[dpfp*]⁺[BF₄][−] 4. A solution of [Cu(NCCH₃)₄]⁺[BF₄][−] (504 mg, 1.60 mmol) and dpfp* (362 mg, 0.80 mmol) in dichloromethane (25 cm³) was stirred for 14 h. Volatile components were removed *in vacuo*. The dark residue was dissolved in the minimum volume of dichloromethane. Vapour-phase diffusion of diethyl ether into this solution afforded complex **4** (293 mg, 68%) as dark green needles (Found: C, 61.9; H, 6.2; N, 5.1. C₂₈H₃₂BF₄FeN₂ requires C, 62.4; H, 6.0; N, 5.2%).

Acknowledgements

B. N., U. S., H.-G. S. and U. V. are grateful to the Deutsche Forschungsgemeinschaft, the Fonds der Chemischen Industrie and the Universität Bielefeld for financial support.

References

- 1 *Ferrocenes*, eds. A. Togni and T. Hayashi, VCH, Weinheim, 1995.
- 2 (a) U. Siemeling, U. Vorfeld, B. Neumann and H.-G. Stammler, *Chem. Commun.*, 1997, 1723; (b) H. Plenio and D. Burth, *Organometallics*, 1996, **15**, 4054; (c) W.-Y. Wong and W.-T. Wong, *J. Chem. Soc., Dalton Trans.*, 1996, 3209; (d) T. Moriuchi, I. Ikeda and T. Hirao, *J. Organomet. Chem.*, 1996, **514**, 153; (e) T. Moriuchi, I. Ikeda and T. Hirao, *Inorg. Chim. Acta*, 1996, **248**, 129; (f) B. König, O. Möller and H. Zieg, *J. Prakt. Chem.*, 1996, **338**, 549; (g) W. R. Thiel, T. Priermeier, D. A. Fiedler, A. M. Bond and M. R. Mattner, *J. Organomet. Chem.*, 1996, **514**, 137; (h) J. G. P. Delis, P. W. N. M. van Leeuwen, K. Vrieze, N. Veldman, A. L. Spek, J. Fraanje and K. Goubitz, *J. Organomet. Chem.*, 1996, **514**, 125.
- 3 N. Sachsinger and C. D. Hall, *J. Organomet. Chem.*, 1997, **531**, 61; E. C. Constable, A. J. Edwards, R. Martínez-Máñez and P. R. Raithby, *J. Chem. Soc., Dalton Trans.*, 1995, 3253; I. R. Butler,

- S. J. McDonald, M. B. Hursthouse and M. A. Malik, *Polyhedron*, 1995, **14**, 529.
- 4 (a) F. Fabrizi de Biani, F. Jäkle, M. Spiegler, M. Wagner and P. Zanello, *Inorg. Chem.*, 1997, **36**, 2103; (b) N. Chabert-Couchoudron, C. Marzin and G. Tarrago, *New J. Chem.*, 1997, **21**, 355; (c) A. K. Burrell, W. Campbell and D. L. Officer, *Tetrahedron Lett.*, 1997, **38**, 1249; (d) E. Herdtweck, F. Jäkle, G. Opromolla, M. Spiegler, M. Wagner and P. Zanello, *Organometallics*, 1996, **15**, 5524; (e) R. J. Less, J. L. M. Wicks, N. P. Chatterton, M. J. Dewey, N. L. Cromhout, M. A. Halcrow and J. E. Davies, *J. Chem. Soc., Dalton Trans.*, 1996, 4055; (f) I. R. Butler, D. S. Brassington, R. A. Bromley, P. Licence and J. Wrench, *Polyhedron*, 1996, **15**, 4087; (g) N. M. Loim, N. V. Abramova and V. I. Sokolov, *Mendeleev Commun.*, 1996, 46.
 - 5 U. Siemeling, U. Vorfeld, B. Neumann and H.-G. Stammer, *Chem. Ber.*, 1995, **128**, 481.
 - 6 K. Tani, T. Mihan, T. Yamagata and T. Saito, *Chem. Lett.*, 1991, 2047.
 - 7 (a) I. Sanyal, K. D. Karlin, R. W. Strange and N. J. Blackburn, *J. Am. Chem. Soc.*, 1993, **115**, 11 259; (b) A. Habiyakare, E. A. C. Lucken and G. Bernadelli, *J. Chem. Soc., Dalton Trans.*, 1991, 2269; (c) M. Munakata, S. Kitagawa, H. Shimono and H. Masuda, *Inorg. Chim. Acta*, 1989, **158**, 217; (d) P. C. Healy, J. D. Kildea, B. W. Skelton and A. H. White, *Aust. J. Chem.*, **42**, 115.
 - 8 B. J. Hathaway, in *Comprehensive Coordination Chemistry*, eds. G. Wilkinson, R. D. Gillard and J. A. McCleverty, Pergamon, Oxford, 1987, vol. 5, pp. 534–774.
 - 9 E. R. Brown and J. R. Sandifer, in *Physical Methods of Chemistry, Electrochemical Methods*, eds. B. W. Rossiter and J. F. Hamilton, Wiley, New York, 1986, vol. 2, ch. 4.
 - 10 G. Pilloni, G. Valle, C. Corvaja, B. Longato and B. Corain, *Inorg. Chem.*, 1995, **34**, 5910; G. Pilloni, B. Corain, M. Degano, B. Longato and G. Zanotti, *J. Chem. Soc., Dalton Trans.*, 1993, 1777; B. Pilloni and B. Longato, *Inorg. Chim. Acta*, 1993, **208**, 17; P. D. Beer, Z. Chen, M. G. B. Drew, J. Kingston, M. Ogden and P. Spencer, *J. Chem. Soc., Chem. Commun.*, 1993, 1046.
 - 11 A. Bondi, *J. Phys. Chem.*, 1964, **68**, 441.
 - 12 K. Singh, J. R. Long and P. Stavropoulos, *J. Am. Chem. Soc.*, 1997, **119**, 2942.
 - 13 P. Pykkö, *Chem. Rev.*, 1997, **97**, 597; *Unkonventionelle Wechselwirkungen in der Chemie metallischer Elemente*, ed. B. Krebs, VCH, Weinheim, 1992.
 - 14 H. Schmidbaur, *Gold Bull.*, 1990, **23**, 11.
 - 15 P. Pykkö, J. Li and N. Runeberg, *Chem. Phys. Lett.*, 1994, **218**, 133.
 - 16 F. A. Cotton, X. Feng, M. Makusz and R. Poli, *J. Am. Chem. Soc.*, 1988, **110**, 7077.
 - 17 J. Beck and J. Strähle, *Angew. Chem.*, 1985, **97**, 419; *Angew. Chem., Int. Ed. Engl.*, 1985, **24**, 409.
 - 18 K. M. Merz, jun. and R. Hoffmann, *Inorg. Chem.*, 1988, **27**, 2120.
 - 19 C. Kölmel and R. Ahlrichs, *J. Phys. Chem.*, 1990, **94**, 5536.
 - 20 D. E. Harwell, M. D. Mortimer, C. B. Knobler, F. A. L. Anet and M. F. Hawthorne, *J. Am. Chem. Soc.*, 1996, **118**, 2679.
 - 21 P. Pykkö, W. Schneider, A. Nauer, A. Bayler and H. Schmidbaur, *Chem. Commun.*, 1997, 1111.
 - 22 A. Martin and A. G. Orpen, *J. Am. Chem. Soc.*, 1996, **118**, 1464 and refs. therein.
 - 23 P. Zanello, in ref. 1, pp. 317–430.
 - 24 K. Watenpaugh and J. Steward, *ABSCAL. XTAL3.2 Reference Manual*, eds. S. R. Hall, H. D. Flack and J. M. Steward, Lamb, Perth, 1992.
 - 25 P. T. Beurskens, G. Admiraal, G. Beurskens, W. P. Bosman, R. de Gelder, R. Israël and J. M. M. Smits, The DIRDIF 94 program system, Crystallography Laboratory, University of Nijmegen, 1994.
 - 26 A. C. Larson in *Crystallographic Computing*, eds. F. R. Ahmed, S. R. Hall and C. P. Huber, Munksgaard, Copenhagen, 1969, pp. 291–294; W. H. Zachariasen, *Acta Crystallogr., Sect. A*, 1967, **23**, 558.
 - 27 S. R. Hall, G. S. D. King and J. M. Steward, *XTAL3.4 User's Manual*, University of Western Australia, Lamb, Perth, 1995.
 - 28 G. M. Sheldrick, SHELXTL PLUS, Siemens Analytical Instruments, Madison, WI, 1990.
 - 29 G. M. Sheldrick, SHELXL 93, University of Göttingen, 1993.
 - 30 A. Togni, M. Hobi, G. Rihs, G. Rist, A. Albinati, P. Zanello, D. Zech and H. Keller, *Organometallics*, 1994, **13**, 1224.

Received 7th July 1997; Paper 7/04785A